IDŐJÁRÁS

Quarterly Journal of the Hungarian Meteorological Service
Vol. 119, No. 3, July – September, 2015, pp. 337–354

Development, data processing and preliminary results of an urban human comfort monitoring and information system

János Unger*, **Tamás Gál**, **Zoltán Csépe**, **Enikő Lelovics**, **Ágnes Gulyás**

Department of Climatology and Landscape Ecology, University of Szeged
P.O.Box 653, 6701 Szeged, Hungary

*****Corresponding author E-mail:* unger@geo.u-szeged.hu

(Manuscript received in final form April 22, 2014)

Abstract—In this study, the infrastructure development and operation of an urban human comfort monitoring network and information system in Szeged and the related preliminary research results are discussed. The selection of the representative sites of the network is based primarily on the pattern of the local climate zones in and around the city. After the processing of the incoming data (air temperature and relative humidity, as well as global radiation and wind speed), a human comfort index (PET) is calculated from the four meteorological parameters are with a neural network method (MLP), then the measured and calculated parameters interpolated linearly into a regular grid with 500 m resolution. As public information, maps and graphs about the thermal and human comfort conditions appear in 10-minute time steps as a real-time visualisation on the internet. As the preliminary case studies show, the largest intra-urban thermal differences between the LCZ areas in a two-day period occurred in the nocturnal hours reaching even 5 ºC in early spring. In the spatial distribution of human comfort conditions, there are distinct differences in the strength of the loading or favorable environmental conditions between the neighborhoods during the daytime. Finally, the utilization possibilities of the results in the future are detailed.

Key-words: local climate zones (LCZ), representative measurement sites, monitoring network, psychologically equivalent temperature (PET), multilayer perceptron, thermal and human comfort maps, real-time visualization, Szeged, Hungary

1. Introduction

Examination taking place in the field of urban environmental changes due to the large number of people affected is considered as an important task. The urban environments are specific – compared to the natural ones – because of the alteration in land cover and surface geometry characteristics as well as the human activity, which may significantly affect the energy and water balance of the area leading to local-scale climate modifications in the atmosphere of cities. As a result, the so-called *urban climate* develops (e.g., *Oke*, 1987). The residents are affected directly to the alterations taking place in the *urban canopy layer* (a layer of air between the average height of the buildings and the street level). The most significant modification is the change in the thermal environment (the *urban heat island* phenomenon, UHI), as well as in the human bioclimatic (thermal comfort) conditions influenced by the thermal environment and other weather parameters.

The importance of the investigation of these issues is supported that in cases of some of the already loading or unfavorable weather situations, the city still adheres to these effects. For example, at heat wave situations in cities the nocturnal cooling weakens, thus the periods characterized by significant physiological load are extended.

Within larger settlements due to the intra-urban heterogeneity of the physical attributes of the surface, the thermal modifying effect is also different. It can be assumed that in many respects, the interactions between the urban parameters and thermal comfort as well as some elements of the weather phenomena within the city are not yet known sufficiently. These interactions can only be analyzed properly using detailed and long-term (several years) measurements, like detection and analysis of the characteristics of these urban thermal patterns. This analysis can be performed with the help of a *monitoring network* installed representatively and in appropriate density. For automatic monitoring network set up in the urban canopy layer, there can be found some international – mainly U.S., Japan, and Taiwan – examples, while in Europe there are very few of these, and none of them are aimed at the detection of patterns of human comfort conditions. A network began to be build from 1999 on with temperature sensors located from the center in different directions radially in London (*Watkins et al.*, 2002), while in Florence, there is a system with temperature-humidity sensors operating since 2004, whose elements observe the thermal features of the city's various built-up districts (*Petralli et al.*, 2013). The most complex network (utilizing meteorological stations and sensors) so far was started up in 2011 in Birmingham. Its development is now in progress and its elements are installed at higher density in the downtown area while less densely in the outskirts of the city (HiTEmp Project, 2014).

However, obviously it is not a realistic option to establish monitoring stations network to all major urban areas, therefore, in the long run, the presentation and prediction of the prevailing thermal comfort conditions in urban areas only through the proper downscaling of weather forecasting models is possible. Development of such a method, however, is only possible using representative and high resolution measurement data in space and time, as well as parameters characterizing the urban surface and geometry in an appropriate manner. The forecasting of weather processes in urban areas – at least in the structure and functioning of the models used – is similar to the issue of climate change prediction. Because urban areas significantly influence the local climate, in order to estimate the possible outcomes of climate change, these areas should be taken into account. At the same time – as the majority of the world's population already lives in cities –, if the urban areas are implemented to climate models in appropriate manner and they are transposed to the climate models, it will be possible to have correct forecasts for these areas in the future.

In the present paper, we aim to show the principle and practice of the siting and configuration of a representative urban human comfort monitoring system and its data processing. Furthermore, we aim to present the preliminary results related to the spatial distribution of the intra-urban human comfort conditions and their real-time visualization as a public information, and finally, to show the utilization possibilities of the results in the future.

2. Local climate zones (LCZ), station place selection, monitoring network

The main purpose of the LCZ system is the characterization of the local environment around a temperature measurement site in terms of its ability to influence the local thermal climate. Therefore, the number of types is not too large and their separation is based on objective, measurable parameters. LCZs are defined as "regions of uniform surface cover, structure, material, and human activity that span hundreds of meters to several kilometres in horizontal scale" (*Stewart* and *Oke*, 2012). Their names reflect the main characteristics of the types (*Table 1*).

The LCZ types can be distinguished by typical value ranges of measurable physical properties. These properties describe the surface geometry and cover (sky view factor, aspect ratio, fractions of building, pervious and impervious surfaces, height of roughness elements, terrain roughness class) as well as the thermal, radiative, and anthropogenic energy (surface admittance and albedo, anthropogenic heat output) features of the surface. As a result, the LCZ system consists of ten 'built' and seven 'land cover' LCZ types (*Table 1*). Although, originally it was not designed for mapping, mapping of the urban terrain the system can be efficiently used as to determine areas which are relatively homogeneous in surface properties and human activities.

In the context of the LCZ classification system, the UHI intensity is not an "urban-rural" temperature difference (ΔT_{u-r}), but a temperature difference between pairs of LCZ types ($\Delta T_{LCZ\ X-Y}$), that is an inter-zone temperature difference (*Stewart et al.*, 2013). Consequently, the usage of the system allows the objective comparison of the thermal reactions in different areas within a city and between cities (intra-urban and inter-urban comparisons).

Table 1. Names and codes of the LCZ types (after *Stewart* and *Oke*, 2012)

Built types		**Land cover types**	
LCZ 1	compact high-rise	LCZ A	dense trees
LCZ 2	compact mid-rise	LCZ B	scattered trees
LCZ 3	compact low-rise	LCZ C	bush, scrub
LCZ 4	open high-rise	LCZ D	low plants
LCZ 5	open mid-rise	LCZ E	bare rock / paved
LCZ 6	open low-rise	LCZ F	bare soil / sand
LCZ 7	lightweight low-rise	LCZ G	water
LCZ 8	large low-rise		
LCZ 9	sparsely built		
LCZ 10	heavy industry		

2.1. LCZs in Szeged

Szeged is located in the south-eastern part of Hungary (46°N, 20°E) at 79 m above sea level on a flat terrain with a population of 160,000 within an urbanized area of about 40 km^2. The area is in Köppen's climatic region Cfb with an annual mean temperature of 10.4 °C and an annual amount of precipitation of 497 mm (*Unger et al.*, 2001). The study area covers an 11.5 km × 8.5 km rectangle in and around Szeged (*Fig. 1*).

In order to apply the LCZ system in the study area, that is to delineate the types occurring therein, a recently developed automated method was used (*Lelovics et al.*, 2014). *Fig. 1.* shows the obtained seven 'built' and four 'land cover' LCZ types and their pattern in and around Szeged.

2.2. Installed and already existing stations

Within the framework of an EU project (URBAN-PATH Project, 2014) a monitoring network with 23 stations (air temperature, *T* and relative humidity, *RH*) was set up in Szeged. Additionally, data series from the stations of the

Hungarian Meteorological Service (HMS) are added. One of them is at the same place where the station D-1 is located (global radiation, *G* and wind speed, *u*) and the other is at the University of Szeged (station 5-1) (*T*, *RH*, *G*) (*Fig. 2*). Altogether, the whole network consists of 24 measurement sites.

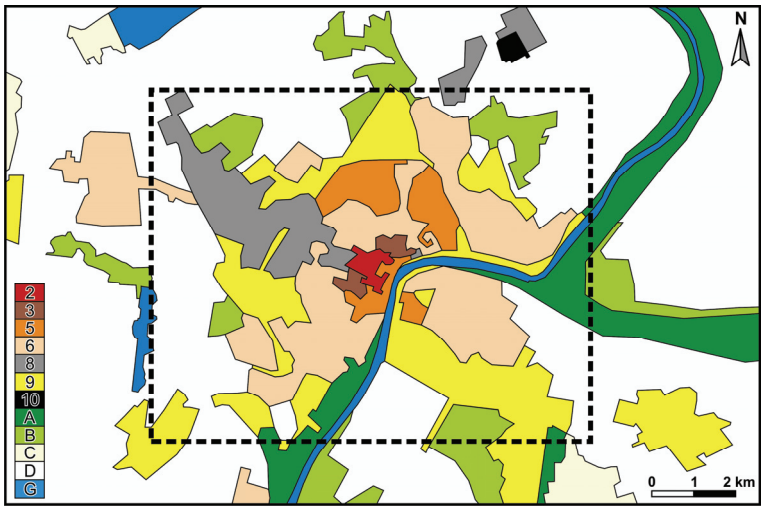

Fig. 1. The obtained LCZ map in Szeged (LCZ 2 – compact mid-rise, LCZ 3 – compact low-rise, LCZ 5 – open mid-rise, LCZ 6 – open low-rise, LCZ 8 – large low-rise, LCZ 9 – sparsely built, LCZ A – dense trees, LCZ B – scattered trees, LCZ C – bush, scrub, LCZ D – low plants, LCZ G – water) and the study area (broken line).

Fig. 2. Station locations of the urban monitoring network in Szeged with their notations (first number indicates the LCZ type, second one indicates the station number in a given LCZ type) (a – station, b – main road, c – water, d – urbanized area) (after *Lelovics et al.* 2014).

In order to have a representative urban human comfort monitoring network within the seven delineated 'built' LCZ areas, the siting and configuration of 22 stations from the above mentioned 24 ones were based on: (i) the distance of the site from the border of the LCZ zone within it was located; (ii) the ability of the selected network geometry to reproduce the spatial distribution of mean temperature surplus pattern estimated by an empirical model (*Balázs et al.*, 2009); (iii) the site's representativeness of its microenvironment; and (iv) the site's suitability for instrument installation. Thus, in summary, two stations (D-1, D-2) represent the rural area, while the other 22 stations the different built-up areas of the city (*Lelovics et al.*, 2014) (*Fig. 2*).

2.3. Measuring equipments

In each monitoring station, the measurement is provided by a Sensirion SHT25 sensor in a radiation protection screen (220×310 mm) at the end of a 60 cm console. The accuracy of the sensor is 0.4 °C and 3% for the temperature and relative humidity, respectively. The radiation protection shield is the same as the model used by the HMS. The consoles are mounted on lamp posts at a height of 4 m above the ground for security reasons. As the air in the urban canyon is well-mixed, the temperature measured at this height is representative for the lower air layers too (but not for the air near the wall or ground) (*Nakamura* and *Oke,* 1988). At the beginning of the console, there are two boxes (*Fig. 3*). The upper one contains the central processor, data storage (microSD) card, GPRS/EDGE/3G modem, battery, and charger. The lower box is utilized in the case of 20 stations where the local electricity provider has made it possible to use the power for the station, and it contains only a separate power switch. At the remaining 4 stations, there is direct access to the power so they do not need any additional boxes.

Fig. 3. One of the stations of the monitoring network on a lamp post (temperature and relative humidity sensors are inside of the radiation shield cylinder).

The system time of the stations (and the whole monitoring system) is in UTC regularly synchronized by the main server. Most of the stations (17 items) have continuous power supply, but seven stations have power supply only when the city lights are on. These seven stations use the power of built in batteries during daytime or at power failure. These stations can operate up to 10 days using only battery power. The stations measure the parameters every minute, and they send the readings with some technical information (battery voltage, temperature inside the box, sensor status) into the main server (Dell PowerEdge T420 tower server) every 10 minutes. If there is no mobile internet connection or the main server does not receive the data, the station tries to send it repeatedly until it succeeded. If the station's battery level is low, the station increases the time between two data transfer to decrease the power consumption. One station (D-1) is located in the garden of the HMS station in order to provide calibration information for the network.

3. Data processing

3.1. Calculation of the human bioclimatological index (PET)

The human (bioclimatological) comfort sensation is formed as the complex effect of air temperature, air humidity, radiation and wind conditions. In order to characterize this comfort sensation, one of the rational indices, the physiologically equivalent temperature (*PET*) is used, which is defined as 'the temperature (in ºC) of a standardized fictitious environment (where the mean radiation temperature is the air temperature, vapor pressure is 12 hPa, and wind speed is 0.1 ms^{-1}), in which the body, in order to maintain its energy balance, gives the same physiological responses like in the complex real-world conditions' (*Mayer* and *Höppe*, 1987).

The PET value categories were initially defined according to thermal sensations and physiological stress levels of Central European people, where the comfortable thermal heat sensation (no stress level) are indicated by a range of 18–23 °C (*Matzarakis* and *Mayer,* 1996). Furthermore, ranges of 13–18 °C and 23–29 °C mean slightly cool and slightly warm sensations, that is slightly cool stress and slightly heat stress levels, respectively, etc.

For the calculation of the PET index, an algorithm, the multilayer perceptron (MLP) network structure (*Haykin*, 1999) was developed (*Fig. 4*). It consists of neurons organized in layers. The neuron's differentiable outputs have non-linearity, which ensure that the output of the network is a continuous differentiable function of the weights. The output layer can be linear or non-linear. Even in the simplest case when an MLP contains only one hidden layer, it implements nonlinear mapping in his parameters. MLP use the error backpropagation learning algorithm, which is an iterative learning process based on an instantaneous gradient.

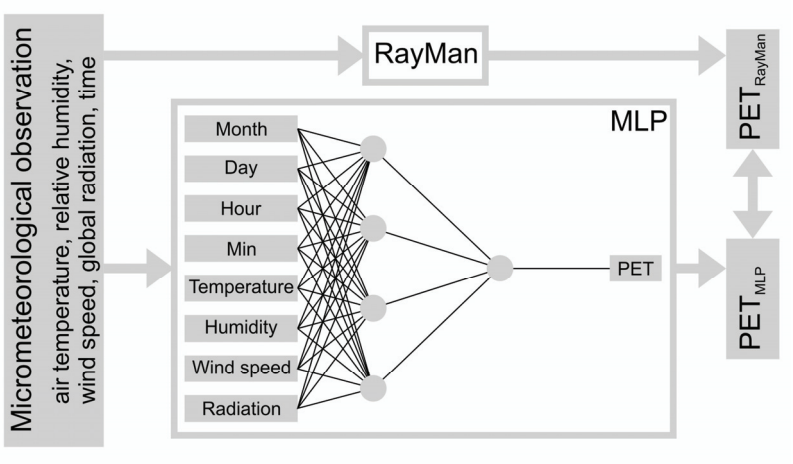

Fig. 4. Flow chart of the development of the MLP

In our case, the input data (air temperature, relative humidity, wind speed, global radiation, time) are derived from the results of the field measurements carried out in different urban microenvironments in Szeged between 2009 and 2013 (e.g., *Kántor* and *Unger,* 2010; *Égerházi et al.*, 2012a, 2012b) (*Fig. 4*). The target output data for the learning was a PET dataset calculated from the same input by the widely used RayMan software (*Matzarakis et al.,* 2007). The MLP model always has one hidden layer and MLP has several parameters that need to be set. They are training time, learning rate, hidden layers, and neurons in the layers. The training time was 1500 epochs, the learning rate started from 0.3 and it was reduced in each step. This helps to stop the network from diverging from the target output as well as to improve the general performance. The number of hidden layers and the nodes in each layer were generated automatically by the WEKA data mining software (*Hall et al.*, 2009). The MLP with these options was applied for predicting the PET index.

3.2. Estimation of the wind and global radiation

For PET calculation in one site in the urban area, the wind speed and radiation data measured there would be ideal. In contrary, if the aim is the monitoring of the thermal comfort conditions in local scale, the direct measurement is not appropriate as the wind speed and radiation measured on site are highly affected by several micro scale phenomena like the arrangement of the nearby obstacles and their effect for the shading and wind flow. Moreover, the deployment of expensive wind and radiation sensors in every urban monitoring site is also not practical because of safety and financial reasons. By virtue of these reasons we used mean wind speed (u_{UCL}) in the urban canopy layer and the undisturbed global radiation (G). The height of the UCL is Szeged in assumed about 30 meters based on the available building database.

As we mentioned, in the study area, the global radiation data are available from the two HMS stations (sites D-1 and 5-1, see Section 2.3). For every monitoring sites, we used the nearest measured global radiation data.

Application of the different forms of logarithmic wind profile (*Oke*, 1987; *Foken*, 2008) for the reduction of the wind speed is prevalent in several thermal comfort studies (*Spagnolo* and *de Dear*, 2003; *Bröde et al.*, 2012). However, this method is questionable if the sum of the roughness length (z_0) and the displacement height (z_d) are higher than the height where we want to calculate the wind speed, because the logarithmic approximation gives 0 ms^{-1} in these cases (*Oke*, 1987; *Foken*, 2008). Therefore, in our study we had to find another solution, because the values of the roughness parameters in urban area (*Gál* and *Unger*, 2009) exceed this limitation. For the estimation of the mean wind speed in UCL, we applied a new method developed for this purpose, however it is mainly based on the power law equation (*Counihan*, 1975):

$$u_1 = u_2 \cdot \left(\frac{z_1}{z_2} \right)^{\alpha}, \tag{1}$$

where u_1 and u_2 are the wind speeds at z_1 and z_2 heights, respectively, and α is estimated as a function of z_0:

$$\alpha \approx \frac{1}{\ln\left(\frac{\sqrt{z_1 \cdot z_2}}{z_0} \right)}. \tag{2}$$

Firstly, we used the Roughness Mapping Tool developed by *Gál* and *Unger* (2013). This is a standalone software for calculation the roughness parameters (z_0, z_d) using building and tree crown database. With this software we calculated z_0 and z_d at the monitoring sites and 8 additional areas. These additional areas are the sites of the earlier thermal comfort studies in Szeged between 2009 and 2012 (*Égerházi et al.,* 2012a, 2012b; *Kántor et al.*, 2011, 2012), and for these areas 59 523 individual wind speed readings are available. We calculated the 10-minute average wind speeds (u_{UCL}) from the 1-minute data of these field measurements and compared them to the 10 minute average wind speed data (u_{10}) from the HMS station. We assumed that u_{UCL} is constant inside the UCL and is equal to u_{10}. Finally, we got 1615 data pairs after filtering out the no- and very weak wind situations ($u < 1$ ms^{-1}).

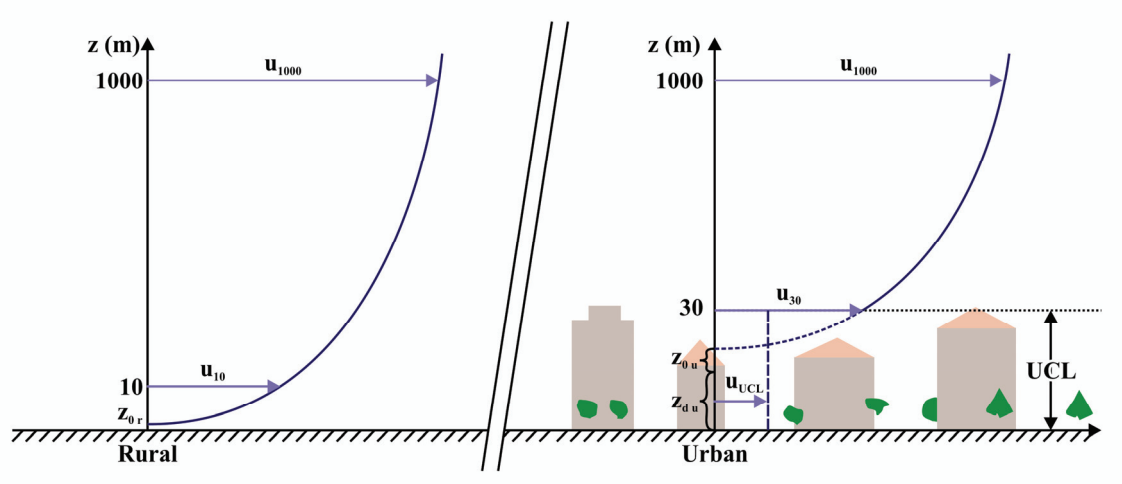

Fig. 5. Concept of the wind speed reduction (for explanation of symbols see the text).

Secondly, the wind speed at a height 1000 m (u_{1000}) was calculated from u_{10} using the logarithmic formula assuming that this u_{1000} value is the regional wind speed unaffected by the drag of the surface (*Fig. 5*). As a next step we determined the wind speed at the top of the UCL (u_{30}) and we calculated a constant (k) with the minimization of the mean square error (MSE) (*Scharf*, 1991) which describes the difference between u_{30} and the measured u_{UCL} (*Fig. 5*). This constant is 0.3331 (MSE=0.3284).

Finally, we obtained the following formula for the wind reduction:

$$u_{UCL} = u_{10} \cdot \left(\frac{1000}{10}\right)^{\alpha_1} \cdot \left(\frac{30 - z_{du}}{1000 - z_{du}}\right)^{\alpha_2} \cdot k \ , \tag{1}$$

where

$$\alpha_1 \approx \frac{1}{\ln\left(\frac{\sqrt{10 \cdot 1000}}{z_{0r}}\right)} \quad \alpha_2 \approx \frac{1}{\ln\left(\frac{\sqrt{(1000 - z_{du}) \cdot (30 - z_{du})}}{z_{0u}}\right)},$$

and subscripts r and u mark the rural and urban sites.

In Equation (1) all value are constants for a given station inside the urban area, except the u_{10} what is measured in the rural station, therefore a complex wind reduction constant (R) was calculated for each monitoring site (*Table 2*) from the constants in this equation. We used this value to calculate the wind speed for the stations from the wind speed measured at D-1 (rural) station at the same time as the time of the PET calculation.

Table 2. Displacement height (z_d), roughness length (z_0), and complex wind reduction constant (R) at urban stations

Station ID	z_d (m)	z_0 (m)	R
2–1	8.7183	1.7455	0.2932
3–1	6.3586	1.4968	0.3116
5–1	6.0872	1.6751	0.3065
5–2	4.6924	2.2986	0.2937
5–3	7.6809	2.0346	0.2887
5–4	5.7750	2.8261	0.2765
6–1	1.7582	0.6740	0.3663
6–2	1.4402	0.4290	0.3856
6–3	1.0717	0.3134	0.3982
6–4	2.6706	0.8682	0.3521
6–5	3.4694	1.0783	0.3392
6–6	3.1466	0.9509	0.3463
6–7	1.5964	0.4782	0.3809
6–8	3.1734	1.1458	0.3372
6–9	1.5275	0.4108	0.3870
6–10	1.2339	0.5226	0.3784
8–1	1.8155	0.2798	0.4001
8–2	2.1910	0.2509	0.4028
9–1	0.1703	0.2000	0.4157
9–2	0.7589	0.2199	0.4111
9–3	0.2805	0.2000	0.4154
9–4	0.7641	0.2177	0.4115

3.3. Operational data processing and display

After the transmission of the station data into the main server every 10 minutes, the automatic data procession system creates the final two (site and spatial) databases (*Fig. 6*) in order to make it possible to present these data as charts and maps on the public homepage of the project (urban-path.hu). Using this public display system, all of the measured and calculated parameters can be accessed a way that the time of the maps and charts can be freely modified by the visitors.

Data received from the monitoring network are stored in one text file per day on the server, and also stored in a MySQL database. Every 10 minutes a Java software calculates the PET value describing the human comfort conditions (see Section 3.1.) for each station using the temperature and relative humidity values measured there, as well as global radiation and wind speed data measured at the

HMS stations (*Fig. 6*). The results of this calculation are also stored in the MySQL database (*Fig. 6*). On the homepage the data, stored in the MySQL database are displayed by charts using PHP scripts.

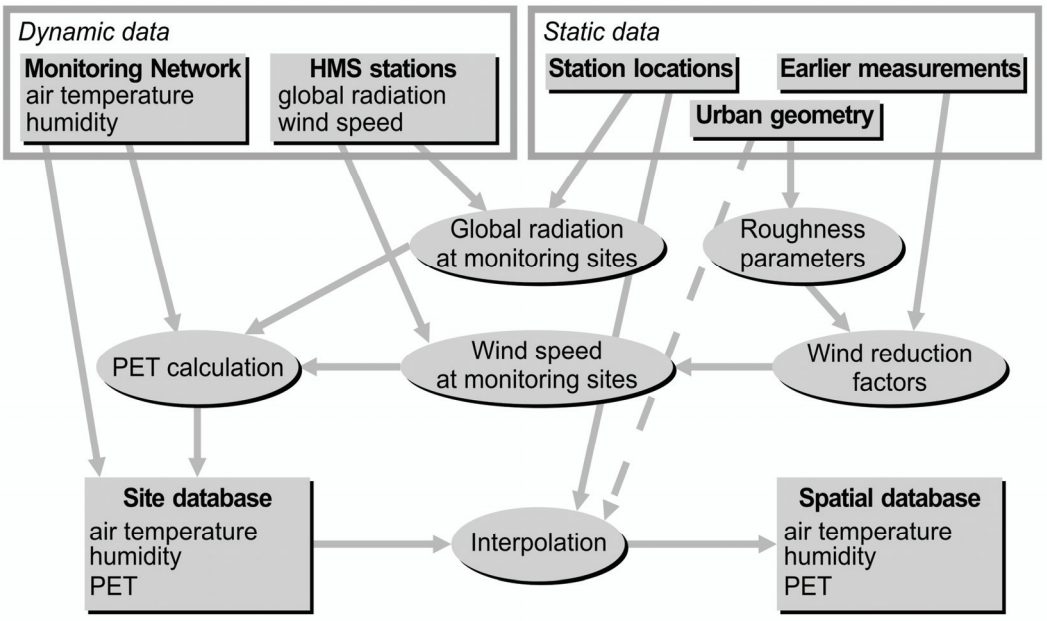

Fig. 6. Flow chart of the automatic data processing of the monitoring system.

For the automatic interpolation of the spatial patterns of the measured and calculated data, a Java software was developed. This program applies simple linear interpolation for a 500 m resolution grid of the study area using the data of the three nearest station of each grid point. In order to avoid the incorrect interpolation in the edge of the study area, the two rural stations are considered as background stations, thus, at the bordering (non-urban) grid points we used the data of the nearest rural station, and all of these points were added to the original measurement points for the interpolation (*Fig. 6*). The coordinates of the grid points and stations are in the Unified Hungarian Projection, but at the end of the interpolation they were converted to WGS84 latitude and longitude coordinates, because it is more appropriate for the further processing (drawing maps with GrADS, comparing the measurements with weather prediction models). At the first hand, we applied a weighting constant (currently it is 1) in the interpolation. After further investigations, we will alter this constant using the statistical connection between the surface parameters (e.g., built-up ratio, SVF, green area, water surface) and the measured temperature, relative humidity, or PET values in order to increase the precision of the interpolation (*Fig. 6*). The final patterns are stored in another, spatial database, which is

technically a NetCDF file. The public project homepage presents these patterns as maps created by GrADS and PHP scripts.

4. Intra-urban variation of the measured and calculated parameters

In this section, the intra-urban differences in the thermal and human comfort conditions are illustrated in selecting time periods, when the weather conditions promoted the microclimatic effects of the spatially varied surface features.

4.1. Temperature data series – comparison of LCZs' thermal reactions

The distinct thermal behavior of the different LCZ areas is shown during a 48 h cloudless period between March 29 and 31, 2014 (from morning to morning) as an example. This period is characterized as a pleasant spring weather. According to the data of the rural HMS station, the insolation was undisturbed during the daylight hours with maximum values of 750–780 Wm^{-2}. The air movement was moderate (0–3 ms^{-1}) except of the first few (daytime) hours (~4–5 ms^{-1}). The days were rather warm with maximum values of 18–20 ºC, but the mornings were a bit chilly with the minimum values of 2–4 ºC because of the intense nocturnal cooling provided by the cloudless sky.

In order to compare the temperature variations of LCZs during the 48 h period, the areal averages were calculated for every LCZ area. As the number of stations located at these areas is different because of the different areal extent of LCZs (from one station in LCZ 2 to ten in LCZ 6, see *Fig. 2*), the *T*-averages are calculated based on original data with different number of sites. As a result seven temperature series are compared ($\Delta T_{LCZ\ X-Y}$), in accordance with the number of LCZs in the study area (except 'heavy industry' (*Fig. 7*).

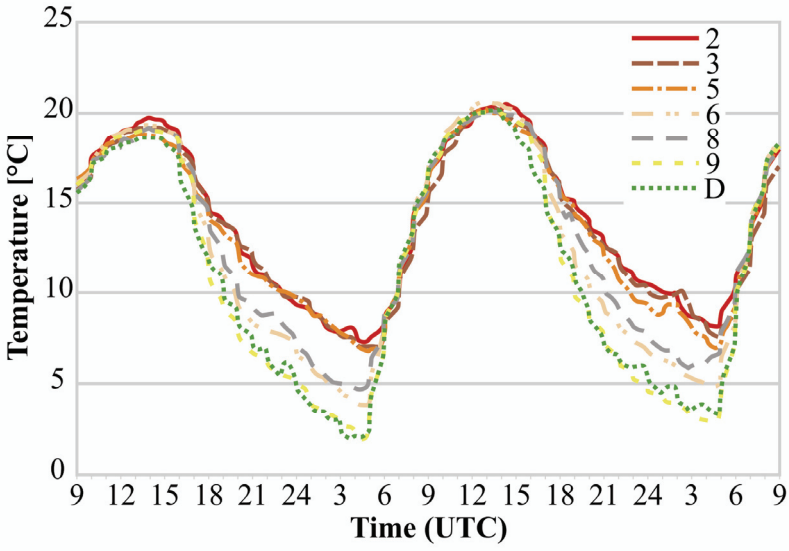

Fig. 7. Temporal variation of the mean LCZ temperatures during a 48 h period (March 29–31, 2014).

As *Fig. 7* shows, the *T*-curves follow the regular shape of the daily temperature cycle in spring, that is warming in the daytime until early afternoon (~8–10 hours) then cooling until dawn (14–16 hours). As expected, LCZ 2 area is the warmest and LCZ 9 and LCZ D types are the coolest, but this is really prevalent at night, as in the daytime the curves move almost together. The largest temperature differences occur in the nocturnal hours: for example, at 4.30 UTC, $\Delta T_{LCZ\ 2–D}$ ~ 5 ºC, $\Delta T_{LCZ\ 5–D}$ ~ 4.5 ºC, but $\Delta T_{LCZ\ 8–D}$ ~ 2,5 ºC only, while $\Delta T_{LCZ\ 9–D}$ ~ 0 ºC at both nights. This can be explained by the slower cooling of the built-up areas compared to the open and more vegetated rural areas because of the radiation processes at the mentioned weather conditions.

4.2. Maps on temperature, relative humidity, and human comfort

During the processing of incoming data (see Section 3), high resolution maps are produced automatically showing the spatial structures of the thermal, humidity, and human comfort conditions, which appear on the project website continuously updated in 10-minute intervals (online) from June 2014.

As an example, in the case of air temperature and relative humidity, we present the situations in the evening hours (*Fig. 8*). That day was also a typical nice spring one with some cloud drift, so the global radiation was a bit disturbed, therefore in the most intensive period, it varied between 550 and 780 Wm^{-2}. The temperature reached 19ºC at the rural HMS station and it was about 10 ºC at 20:00 UTC. The daytime wind speed was 2–3 ms^{-1}, then it decreased to about 1 ms^{-1} in the evening.

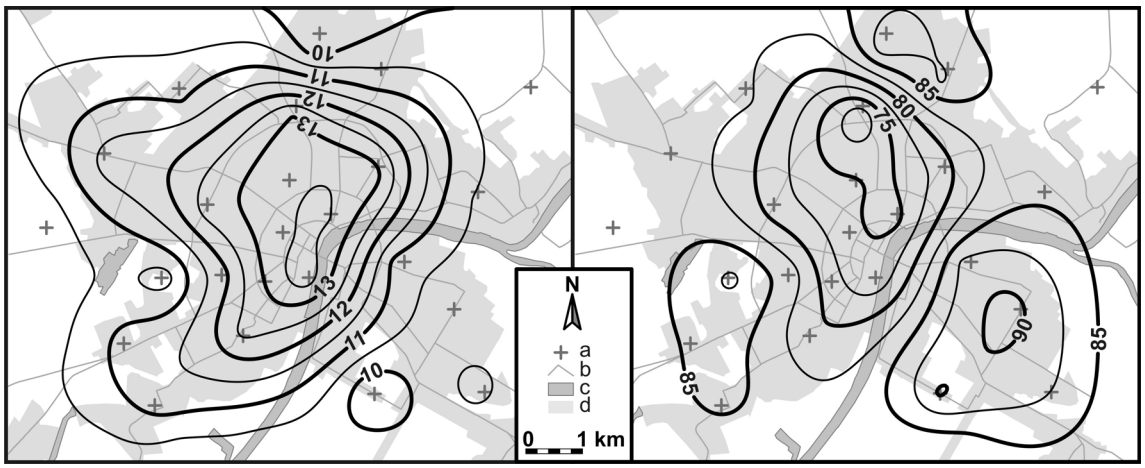

Fig. 8. Intra-urban patterns of temperature (ºC) and relative humidity (%) at 20:00 UTC, April 7, 2014 (a – station, b – main road, c – water, d – urbanized area).

The *T*-pattern shows a typical 'island-like' shape with a maximum of over 13.5 ºC in the inner city. The values decrease toward the outskirts to about 10 ºC (as mentioned above in the case of rural HMS stations). A small deviation from the quasi-concentric shape can be found in the western parts of the city, where small lakes and large green areas are predominant. An opposite case can be experienced for the RH: the largest values (85–90%) occur in the periphery and the smallest ones (under 75%) in the inner parts stretching a bit toward the hosing estates in the north-eastern parts of the city. The shape of the temperature pattern is mostly similar to the results of the previous UHI measurement campaign in Szeged (*Unger et al.*, 2001; *Balázs et al.*, 2009), thus the selection of the sites was really representative.

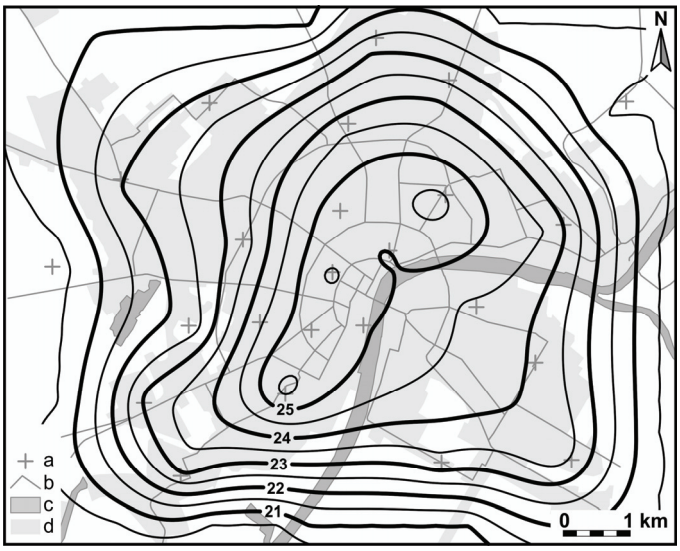

Fig. 9. Intra-urban pattern of human comfort conditions (PET ºC) at 12:00 UTC, April 7, 2014 (a – station, b – main road, c – water, d – urbanized area).

In the case of human comfort conditions, the *PET*-pattern for the daytime (12:00 UTC) is presented. At that time, the distribution of temperature (not shown) is almost homogeneous in the study area (with a variation of less than 0.5 ºC around 17 ºC), but in the *PET* values a range of 20.5–25.5 ºC occurs. Accordingly, there is comfortable thermal heat sensation (no stress level) in outer parts of the city (below 23 ºC *PET*), and much of the city has been experiencing a very slightly warm sensation (slight heat stress level) (from 23 to 25.5 ºC *PET* in the inner parts). Consequently, already in this nice and not too warm early spring day, the environmental conditions in the inner urban parts can be a bit loading for the people. This can be explained by the altered wind conditions (lower wind speeds in the inner urban parts) with rather uniform insolation. This (thermal) load could be strengthened by the fact that after the colder winter days, the thermal contrast (e.g., stronger sunshine) is rather large for the unprepared (not accustomed) people staying outdoors.

5. Conclusions and outlook

Based on this study, the following conclusions can be drawn in accordance with the aims set in Section 1.

Besides the two already existing measurement points, 22 additional sites were selected within the seven delineated local climate zones in Szeged in order to develop a representative urban human comfort monitoring network and information system.

The incoming data (*T*, *RH* from 24 stations, *G*, *T,* and *RH* from the urban HMS station, as well as *G* and *v* from the two HMS stations) were processed by the following steps: firstly, G estimation for each station where it is not measured, then wind reduction for each station using roughness parameters and logarithmic wind profile, and final adjustment using previous street-level wind measurements. Secondly, PET calculation from the four meteorological parameters with a neural network method (MLP) was processed, followed by a linear interpolation of the measured and calculated parameters into a regular grid with 500 m resolution.

As public information, the maps about the thermal and human comfort conditions, and additionally, different graphs about the temporal variations of *T*, *RH*, and PET value appear in 10-minute time steps as a real-time visualization on the project homepage (URBAN-PATH Project, 2014).

According to the preliminary outcomes as case studies, the largest intra-urban thermal differences between the LCZ areas in a two-day period occurred in the nocturnal hours reaching even 5 ºC in early spring. These results confirm the findings of *Stewart* and *Oke* (2012), that is the thermal influence of any change or difference in landscapes (e.g., the different levels of urbanization) are better demonstrated using LCZ difference concept than a simple but generally not clear urban-rural approach, and additionally, it provides an opportunity for intra- and inter-urban comparisons. In the spatial distribution of human comfort conditions, there are distinct differences in the strength of the loading or favorable environmental conditions between the neighborhoods during the daytime. As the inhabitants can meet large differences even within relatively short distances, the urban areas can not be considered homogeneous from this respect.

In summary, as a result of the infrastructure development and related research in the frame of the URBAN-PATH project, an operating urban human comfort monitoring network and information system was established in Szeged.

The utilization possibilities of the results in the future are related to the high-resolution weather prediction models which can be applied in the urban environments – these are real alternatives of urban climate measurement networks –, but their results are not adequate enough so far (*Case et al.,* 2008; *Chen et al.,* 2011; *Salamanca et al*., 2011). Real time predictions of urban meteorological environment are based not only on the attributes of static urban parameters (built-up ratio, sky-view factor, building heights, etc.), because these data are basically constant in the prognostic time-scales. On the other hand, the

actual weather of a given urban region strongly depends on physical processes working in macro- and meso-scales. The mentioned processes can be taken into account only using a well-defined, telescopic downscaling method with the help of a high resolution numerical weather prediction model (such as WRF). Today these high resolution models are directly able to predict the urban meteorological effects and give adequate data for a complex urban weather prediction system. Nevertheless, the basic urban surface data sets and their attributes which are needed to make a successful forecast will have to be specified. Since the urban weather factors mainly work on meso-γ and micro-α scales, the applied numerical model will be able to run with 300 m horizontal resolution and dense vertical layering. Based on the mentioned challenges, it is important to implement a high-resolution urban static database into the WRF system moreover, the global and local (urban) meteorological data assimilation procedures are required. An WRF-based urban meteorological prediction system can be able to give fundamental data for some new research aspects such as military, urban planning, public health, etc., applications.

Acknowledgements: The study was supported by the Hungary-Serbia IPA Cross-border Co-operation Programme (HUSRB/1203/122/166 – URBAN-PATH), in case of the second author by the Hungarian Scientific Research Fund (OTKA PD-100352) and by the János Bolyai Research Scholarship of the Hungarian Academy of Sciences, and in case of the fourth author by the TÁMOP 4.2.4. A/2-11-1-2012-0001 „National Excellence Program – Elaborating and operating an inland student and researcher personal support system convergence program", which project was subsidized by the EU and co-financed by the European Social Fund.

References

Balázs, B., Unger, J., Gál, T., Sümeghy, Z., Geiger, J., and *Szegedi, S.*, 2009: Simulation of the mean urban heat island using 2D surface parameters: empirical modeling, verification and extension. *Meteorol. Appl. 16,* 275–287.

Bröde, P., Fiala, D., Błażejczyk, K., Holmér, I., Jendritzky, G., Kampmann, B., Tinz, B., and *Havenith, G.,* 2012: Deriving the operational procedure for the Universal Thermal Climate Index (UTCI). *Int. J. Biometeorol. 56*, 481–494.

Case, J., Crosson, W., Kumar, S.V., Lapenta, W.M., and *Peters-Lidard, C.D.*, 2008: Impacts of high-resolution land surface initialization on regional sensible weather forecasts from the WRF model. *J. Hydromet. 9*, 1249–1266.

Chen, F., Kusaka, H., Bornstein, R., Ching, J., *Grimmond, C.S.B., Grossman-Clarke, S., Loridan, T., Manning, K.W., Martilli, A., Miao, S., Sailor, D., Salamanca, F.P., Taha, H., Tewari, M., Wang, X., Wyszogrodzki, A.A.,* and *Zhang, C.,* 2011: The integrated WRF/urban modelling system: development, evaluation, and applications to urban environmental problems. *Int. J. Climatol. 31*, 273–288.

Counihan, J., 1975: Adiabatic atmospheric boundary layers: A review and analysis of data from the period 1880-1972. *Atmos. Environ. 9,* 871–905.

Égerházi, L., Kántor, N., Takács, Á., and *Unger, J.*, 2012a: Patterns of attendance and thermal conditions on a pedestrian street. Proceed of the 8th Int. Conf. on Urban Climate. Dublin, Ireland, Paper no. 170.

Égerházi, L., Kántor, N., Takács, Á., Gál, T., and *Unger, J.*, 2012b: Thermal stress maps validation with on-site measurements in a playground. Proceed of the 8th Int. Conf. on Urban Climate. Dublin, Ireland, Paper no. 169.

Foken, T., 2008: Angewandte Meteorologie. Springer, Berlin–Heidelberg.
Gál, T. and *Unger, J.*, 2009: Detection of ventilation paths using high-resolution roughness parameter mapping in a large urban area. *Build. Environ. 44*, 198–206.
Gál, T. and *Unger, J.,* 2013: Calculation of the aerodynamical roughness parameters using building and tree-crown database. In (eds: *Pajtókné Tari I, Tóth A.)* Changing Earth, Changing Society, Changing Learning – The role of renewable energy in regional development Int. Conf. Eger, Hungary, 43–48.
Hall, M., Frank, E., Holmes, G., Pfahringer, B., Reutemann, P., and *Witten, I.H.*, 2009: The WEKA data mining software: an update. *ACM SIGKDD Explorations Newsletter 11*, 10–18.
Haykin, S., 1999: Neural Networks: a comprehensive foundation (2nd ed.). Prentice Hall, Upper Saddle River, NJ.
HiTemp Project, 2014: High Density Measurements within the Urban Environment. http://www.birmingham.ac.uk/schools/gees/centres/bucl/hitemp/index.aspx. Last accessed: April 10, 2014.
Kántor, N. and *Unger, J.,* 2010: Benefits and opportunities of adapting GIS in thermal comfort studies in resting places: An urban park as an example. *Landsc. Urban Plan. 98,* 36–46.
Kántor, N., Gulyás, Á., Égerházi, L., and *Unger, J.,* 2011: Assessments of the outdoor thermal conditions in Szeged, Hungary: thermal sensation ranges for local residents. In (eds: *Gerdes, A., Kottmeier, C.* and *Wagner, A*.) Climate and Construction Int. Conf. Karlsruhe, Germany, 181–190.
Kántor, N., Égerházi, L., and *Unger, J.*, 2012: Subjective estimation of thermal environment in recreational urban spaces—Part 1: investigations in Szeged, Hungary. *Int. J. Biometeorol. 56,* 1075–1088.
Lelovics, E., Unger, J., Gál, T., and *Gál, C.V.,* 2014: Design of an urban monitoring network based on Local Climate Zone mapping and temperature pattern modeling. *Climate Res.* (doi: 10.3354/cr01220)
Matzarakis, A. and *Mayer, H.,* 1996: Another kind of environmental stress: thermal stress. *WHO Newsletter 18,* 7–10.
Matzarakis, A., Rutz, F. and *Mayer, H.,* 2007: Modelling radiation fluxes in simple and complex environments—application of the RayMan model. *Int. J. Biometeorol. 51,* 323–334.
Mayer, H. and *Höppe, P.,* 1987: Thermal comfort of man in different urban environments. *Theor. Appl. Climatol. 38,* 43–49.
Nakamura, Y. and *Oke, T.R.,* 1988: Wind, temperature and stability conditions in an east-west oriented urban canyon. *Atmos. Environ. 22,* 2691–2700
Oke, T.R., 1987: Boundary Layer Climates. (2nd ed.) Routledge, University Press, Cambridge.
Petralli, M., Masetti, L., Brandani, G., and *Orlandini, S.,* 2013: Urban planning indicators: useful tools to measure the effect of urbanization and vegetation on summer air temperatures. *Int. J. Climatol. 34,* 1236–1244.
Salamanca, F., Martilli, A., Tewari, M., and *Chen, F.,* 2011: A study of the urban boundary layer using different urban parameterizations and high-resolution urban canopy parameters with WRF. *J. Appl. Meteorol. Climatol. 50*, 1107–1128.
Scharf, L.L., 1991: Statistical signal processing. Vol. 98. Reading, MA: Addison-Wesley.
Spagnolo, J. and *de Dear, R.,* 2003: A human thermal climatology of subtropical Sydney. *Int. J. Climatol. 23*, 1383–1395.
Stewart, I.D. and *Oke, T.R.,* 2012: Local Climate Zones for urban temperature studies. *Bull. Am. Meteorol. Soc. 93,* 1879–1900.
Stewart, I.D., Oke, T.R., and *Krayenhoff, E.S.,* 2014: Evaluation of the 'local climate zone' scheme using temperature observations and model simulations. *Int. J. Climatol. 34,* 1062–1080.
Unger, J., Sümeghy, Z., Gulyás, Á., Bottyán Z. and *Mucsi, L.*, 2001: Land-use and meteorological aspects of the urban heat island. *Meteorol. Appl. 8,* 189–194.
URBAN-PATH Project, 2014: Evaluations and Public Display of Urban Patterns of Human Thermal Conditions. http://urban-path.hu/. Last accessed: April 20, 2014.
Watkins, R., Palmer, J., Kolokotroni, M. and *Littlefair, P.,* 2002: The London heat island: Results from summertime monitoring. *Build. Serv. Eng. Res. Technol. 23,* 97–106.